Proceedings of the Pakistan Academy of Sciences: A Physical and Computational Sciences 61(4): 349-359 (2024)

ISSN (Print): 2518-4245; ISSN (Online): 2518-4253
http://doi.org/10.53560/PPASA(61-4)685

Pakistan Academy of Sciences

Research Article

Study of Newly Synthesized Pyridinium-based Cationic Surfactants for Drug Interaction and Antibacterial Activity

Ali Jaan[1,2], Saqib Ali[2], Mohsin Javed[1], Ali Haider[2], Khurram Shahzad Munawar[3,4]*, Saja Abdulrahman Althobaiti[5], and Mahboob ur Rehman[6]

[1]Department of Chemistry, School of Science, University of Management and Technology, C-II Johar Town, Lahore, Pakistan

[2]Department of Chemistry Quaid-i-Azam University, 45320, Islamabad, Pakistan

[3]Institute of Chemistry, University of Sargodha, Sargodha, 40100, Pakistan

[4]Department of Chemistry, University of Mianwali, Mianwali, 42200, Pakistan

[5]Department of Chemistry College of Sciences and Humanities, Prince Sattam Bin Abdulaziz University, Saudi Arabia

[6]Cardiology Department, Pakistan Institute of Medical Sciences (PIMS), Islamabad, Pakistan

Abstract: Two pyridinium-based new cationic surfactants have been synthesized by the reaction of 2-methylpyridine and 3-methylpyridine with an alkyl halide (1-bromoctadecane) using dry toluene as a solvent to get the compounds, N-(n-octadecyl)-2-methylpyridinium bromide (A1) and N-(n-octadecyl)-3-methylpyridinium bromide (A2), respectively. The synthesized samples were characterized by using various spectroscopic techniques. The synthesized compounds showed a critical micelle concentration in a very low-value range (0.111 mM to 0.125 mM), proving the synthesized compounds' best surface-acting ability. Both compounds exhibited limited antibacterial activity across various bacterial strains, with inhibition zones ranging from 3 to 7 mm. The change in Gibb's free energy (ΔG) was also calculated from their binding constant (K_b) for samples A1 **(**-10.0 kJ/mol) and A2 **(**-19.37 kJ/mol). The samples demonstrated spontaneous interactions with the drug molecules, which proved the efficient bioavailability of the drug due to the best incorporation of drug molecules with the aggregated monomers of surfactant molecules.

Keywords: Pyridinium, Cationic Surfactants, Drug Delivery, Antibacterial Activity, Spectroscopic Techniques.

1. INTRODUCTION

Recent advancements in the development and application of surfactants have been notable, driven by a focus on improving their performance [1-3]. These innovations in surfactant production are unlocking new opportunities for their use across various scientific disciplines, leading to more efficient and effective solutions in areas such as chemistry, materials science, and industrial applications [4-8]. Although the surfactants' study has become a considerable field of science, an uninterrupted regulation of environment-friendly consumer products is still needed, by developing new molecules, tailored for the required purposes and applications explicitly. Especially, the compounds of cationic surfactants are a class in which the nitrogen atom (of the pyridine ring in the case of pyridinium-based surfactant) possesses a positive charge, which is referred to as the tail of a compound, directly linked to the alkyl head group. This framework makes them cleavable (i.e., also named cleavable surfactants) because their properties are easily reformed from surface-acting agents to non-active agents by the decomposition process making them an efficient biodegradable

Received: October 2024; Revised: November 2024; Accepted: December 2024
* Corresponding Author: Khurram Shahzad Munawar <khurramchemist@gmail.com>

agent. Alongside, they exhibit germicidal properties as sanitizing agents, static-free agents, corrosion-inhibiting agents, and inter-fiber friction-reducing agents [9, 10]. Surfactants are so named due to their role as surface-active agents, a term that reflects their bioavailability and ability to interact with surfaces [11, 12].

The nature of surfactant molecules is inorganic as they show amphiphilic characteristics. Therefore, they contain a hydrophilic polar head group and a hydrophobic non-polar tail group showing water-soluble and water-insoluble properties, allowing the comparison of solubilities even with the seawater [13-15]. In this regard, when surfactant molecules migrate toward the surface of the water, the hydrophobic part goes on to the air or into the oil phase. If water is mixed with the oil, the polar part is simply retained in the water phase [16]. The aggregation as well as the positioning of the different groups of the surfactant molecules enables the surfactants to change the surface properties of water at different interfaces including water-oil/water-air interfaces [17, 18]. For instance, the decline in the aggregation property of surfactants, regarding their micellization, is due to the salt incorporation having bromide ion as an anionic radical [19-21]. The general and bio-related surfactants are divided into various fields of science regarding their applicability in daily life as well as in vast medical fields, including nucleic acid delivery, etc. [22-25]. In nitrogen-based cationic surfactants, a head group is considered a hydrophilic polar nature part, soluble in water. In contrast, the tail group, which is more often thought to be a long chain of alkyl nonpolar hydrophobic parts, is insoluble in water [26].

The proper and controlled release of drugs is mandatory for drug therapy to living organisms more likely to humans [27]. In most cases, non-uniform drug concentration release is observed and the solution of this proposed remedy is crucial. To avoid the inimical effect produced by the high-concentration delivery to the non-targeted spot and low concentration to the targeted spot, the controlled delivery of the drug is demanded [28, 29]. More often the hydrophobic nature of drugs used for the drug delivery phenomenon is intended to decrease the degradation of the drug and the detrimental effects with the efficient bio-availability on the required site of the body because of the drug's less solubilization property [30, 31]. Another major problem regarding to use of cationic or anionic drugs is the transformation of the structure of the cell membrane, which leads to the disturbance in the proper functioning of cells because the drugs cannot easily cross the cell membrane of living organisms. The complete therapy needs an excess amount of drug, which results in toxicity as well as the aggregation of drugs on non-target sites [32].
The present study is accompanied by the use of broadly used surfactants prepared by the derivatives of pyridine. The newly prepared compounds, followed by the use of the aggregation properties of monomers, are used for the efficient delivery of a required drug to the target site of the living body. The aggregation of the molecules leads to the micellization phenomenon, which provides the basic environmental needs for drug encapsulation as well as its safe delivery [33].

2. MATERIALS AND METHODS

2.1. Chemicals

All chemicals, such as alkyl halide, 2-methyl pyridine, 3-methylpyridine, and solvents, such as toluene, chloroform, methanol, ethanol, n-hexane, diethyl ether, ethyl acetate, and DMSO, used in the current work, were of analytical grade and purchased from Sigma-Aldrich and Alfa-Aesar.

2.2. Instrumentation

A Sanyo electro-thermal melting point apparatus was used for the melting point determination of the synthesized compounds with the help of an open capillary tube. A 3000MX model of Bio-Rad Excalibur was used for recording the FT-IR absorption spectra using KBr pallets in the range of 4000-400 cm^{-1} [34]. A 300 MHz-FT-NMR of Bruker AC was used to take ^{1}H-NMR & ^{13}C-NMR spectra in deuterated solvent ($CDCl_3$). The chemical shift of various bonds was denoted with δ and given in parts per million (ppm). The structures of newly synthesized cationic surfactants were confirmed by FT-IR, ^{1}H-NMR, and ^{13}C-NMR spectroscopies. The peaks for C-N in the samples A1 and A2 were observed at 1170 cm^{-1} and 1209 cm^{-1}, respectively, in FT-IR spectra. Similarly, the signals for C-N moiety in ^{1}H NMR can be seen at 58.56 ppm and 61.98 ppm for samples A1 and A2, respectively. The determination of critical micelle concentration

(CMC) followed by the drug interaction study was carried out using a spectrophotometer (Shimadzu) equipped with a UV lamp (SN:500412). The electrical conductivities also followed by the critical micelle concentration (CMC) of synthesized compounds were performed by the conductometer of Inolab 720 precision conductivity meter at room temperature.

2.3. Synthesis of Cationic Surfactants (A1 and A2)

The surfactants were prepared by reacting 5.20 mL of 1-bromoctadecane (0.020 moles) with 1.97 mL (0.020 moles) of 2-methylpyridine (for A1) and 3-methylpyridine (for A2), in 40 mL of dry toluene, separately. The reaction media were kept on a hot plate under the refluxing environment with continuous stirring for 12 hours until the brownish precipitates of A1 and white precipitates of A2 appeared from their respective media. After cooling, these precipitates were stirred with 50 mL of diethyl ether for 2-3 hours to remove the unreacted precursors. The precipitates were collected using filtration and finally dried in air. The general procedure for the synthesis of both samples and the carbon numbering pattern for NMR studies is shown in Scheme 1.

A1: Yield: 90 %; Molecular formula = $C_{24}H_{44}NBr$; Molecular mass = 426.4 g/mol; Physical state = Solid; Color = Brown: Melting Point = 123 °C: Solubility = Ethanol, Methanol, Acetone, DMSO, Chloroform; CMC at 298.16 K = 0.1255 (mmol/dm^3): FT-IR (400-4000 cm^{-1}), C-N = 1170, C=N = 1632, C=C = 1574, -CH_2 (Aliphatic) = 1466, CH (Aromatic) = 3039, CH_3 = 1142. ^{1}H-NMR (300 MHz, $CDCl_3$, δ-ppm): 9.61 (1H, H^5, d, ^3J = 5.7 Hz), 8.42 (1H, H^4, t, ^3J = 7.8 Hz), 7.997 (1H, H^3, t, ^3J = 3.6 Hz), 4.88 (2H, H^7, t, ^3J = 7.8 Hz), 2.98 (3H, H^6, s), 0.844-2.980 (37H, H^{8-24}, m). ^{13}C-NMR (75.5 MHz, $CDCl_3$, δ-ppm): 154.19 (C^1), 146.66 (C^2), 145.14 (C^3), 130.26 (C^4), 126.43 (C^5), 26.31 (C^6), 58.56 (C^7), 14.1-34.0 (C^8-C^{24}).

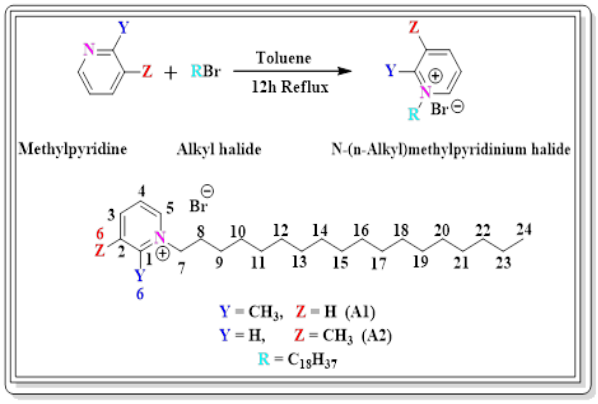

Scheme 1: Conversion of methylpyridine to N-(n-Alkyl) methylpyridinium halide (A1 and A2) and numbering pattern for NMR results.

A2: Yield: 95 %; Molecular formula = $C_{24}H_{44}NBr$; Molecular mass = 426.4 g/mol; Physical state = Solid; Color = White; Melting Point = 118 °C; Solubility = Ethanol, Methanol, Acetone, DMSO, Chloroform; CMC at 298.16 K = 0.1174 (mmol/dm^3); FT-IR (400-4000 cm^{-1}), C-N = 1209, C=N = 1633, C=C = 1590, -CH_2 (Aliphatic) = 1470, CH (Aromatic) = 3033, CH_3 = 1146; ^{1}H-NMR (300 MHz, $CDCl_3$, δ-ppm): 9.324 (1H, H^1, s), 9.216 (1H, H^5, d, ^3J = 5.7 Hz), 8.272 (1H, H^3, d, ^3J = 8.1 Hz), 8.027 (1H, H^4, t, ^3J = 7.5 Hz), 2.62 (3H, H^6, s), 4.92 (2H, H^7 t, ^3J = 7.2 Hz), 0.894-4.948 (37H, H^{8-24}, m). ^{13}C-NMR (75.5 MHz, $CDCl_3$, δ-ppm): 145.61 (C^1), 144.51 (C^2), 142.27 (C^3), 139.64 (C^4), 127.80 (C^5), 26.11 (C^6), 61.98 (C^7), 18.78-34.11 (C^8-C^{24}).

2.4. Determination of Critical Micelle Concentration (CMC)

The evaluation of critical micelle concentration was performed by conductometry and UV-Visible spectrophotometry.

2.4.1. Conductometry

Several different dilutions were prepared and tested by the conductometer, (equipped with a conductivity cell) calibrated by KCl, to check the conductivity of the surfactant-containing solution. Upon dilution with ethanol, the conductivity decreases and a clear change in the values of conduction was observed. The temperature was kept at 25.0 ± 0.1 °C due to the activity.

2.4.2. UV-Visible spectrophotometry

A series of different dilutions were prepared from a 25 mL stock solution of 0.3 M. Then, 1.3 mL was taken from the stock solution and diluted with the help of ethanol up to 2.6 mL to make the solution 0.15 M. To analyze the absorption data of the synthesized surfactants at different concentrations, 13 readings were taken for each 0.1 mL dilution using a micropipette. The dilutions were

prepared similarly to those used in conductivity measurements.

A double-beam spectrophotometer 1800 Shimadzu, having a scanning speed range from 200 to 800 nm was used for the measurement of absorption spectra using quartz cells with a path length of 1 cm. At the start, both cells were filled with 3/4th of solvent (Ethanol) for the baseline auto-zero correction. Then the sample cell was filled with the surfactant-containing a solution of a known concentration of 0.3 M, which was later on diluted to 0.15 M, to record the spectra.

2.5. Drug-Surfactant Interaction

The interaction of synthesized surfactants with the drug was carried out by taking the solution of the drug with a constant concentration in ethanol and interacting it with the variable concentrations (as discussed in the previous section) of surfactants, i.e., from pre-micellar to the post-micellar region. Initially, both cells were filled with solvent, for the auto-zero baseline correction. Consequently, a surfactant solution of different concentrations that are formed for the pre- to post-micellar region was mixed with the drug solution with its constant concentration. All the spectra of surfactant, with the drug, before and after CMC, were recorded.

2.6. Antibacterial Studies

The antibacterial activity was performed against *Staphylococcus aureus*, *Staphylococcus pseudo*, and *Klebsiella pneumoniae* bacterial strains. The bacterial cultured plates were prepared by dissolving Broth and Agar in deionized water in a flask and then autoclaved for 20 minutes. After cooling down the solution, a bacterial strain was introduced to the flask to prepare the inoculum. All three inoculums of bacteria were prepared following the same procedure and kept the inoculums for 24 hours in a shaker at a constant temperature. The already sterilized petri dishes were filled with the prepared solution of Agar and Broth. Then three bacterial strains were introduced separately into the prepared petri dishes. Then the positive and negative controls were added along with the sample and Gentamicin (standard drug) into the different zones of petri dishes and were placed into the incubator carefully for 24 hours. The bacterial strains showed the scavenging areas, which were noted down.

3. RESULTS AND DISCUSSION

3.1. Structural Elucidation

3.1.1. Fourier transform infrared (FT-IR) spectroscopy

The details of the spectral peaks are shown in the experimental section and FT-IR spectra of both samples A1 and A2 are shown in Supplementary Figures S1 and S2 (all Supplementary Figures can be accessed at: https://ppaspk.org/index.php/PPAS-A/article/view/1529/862). Generally, FT-IR spectroscopy exploits the fact of structural elucidation using functional group and type of bond determination. The assigned peaks to different types of bonds and various functional groups present in newly synthesized surfactants are accomplished through a literature review [35, 36]. The attachment of the pyridine ring to the long alkyl chain can be seen using the C-N bond, which is in the range of 1050-1200 cm^{-1}. A range of 717-728 cm^{-1} is purely associated with the hydrocarbon chain length. The peaks for the C=N of sample A1 can be seen at 1632 cm^{-1} and for the sample A2, it is visible at 1633 cm^{-1}. Moreover, the C-N peaks for samples A1 and A2 can be observed at 1170 cm^{-1} and 1209 cm^{-1}, respectively. The stretching peaks for the alkyl chain of aliphatic –CH_2, for samples A1 and A2, can be spotted at 1466 cm^{-1} and 1470 cm^{-1}, respectively. However, the aromatic –C-H, stretching peak usually appears slightly above 3000 cm^{-1}. So, for sample A1, it can be seen at 3039 cm^{-1}, and for sample A2, it is at 3033 cm^{-1}. The appearance of these peaks confirms the successful synthesis of above discussed new compounds and is in good agreement with the relevant literature [37-39].

3.2. Nuclear Magnetic Resonance (NMR) Spectroscopy

The details of the spectral peaks are shown in the experimental section and the spectra of both samples are shown in Figures S3-S6. In the case of ^{1}H-NMR, a signal for -H_2C-$N_{(pyridine)}$ at 4.880 ppm for A1, and a signal for 4.924 ppm for A2 confirm the synthesis of samples. Furthermore, in the case of ^{13}C-NMR, the confirmatory signal due to -H_2C-$N_{(pyridine)}$ moiety was observed at 58.56 ppm and 61.98 ppm for samples A1 and A2, respectively. In the ^{13}C-NMR, the peaks for aromatic carbons (C1-C5) of sample A1 are visible at 154.19, 146.66,

145.14, 130.26, and 126.43 ppm, respectively. Meanwhile, the peaks for the aliphatic carbon chain can be seen in the 14.12-31.91 ppm range. For sample A2, the signal for aromatic carbons (C1-C5) can be seen at 145.61, 144.51, 142.27, 139.64, and 127.80, respectively. The peaks for the aliphatic carbon chain can be seen in the range of 18.78-34.11 ppm. The peak for the methyl carbon attached to the aromatic ring appears at 26.31 and 26.11 ppm for samples A1 and A2, respectively. Both samples acquired chemical shift values that nearly match the stated chemical shifts in the literature [3, 40, 41].

3.3. Determination of CMC by Conductometry

For conductometric measurements of the synthesized compounds, the standard solutions were prepared in ethanol at 298 K. A graph was plotted against the concentration taken on abscissa and conductivity on the y-axis. A point where the accumulation of surfactant monomers started was of actual interest while discussing the graph, which is generally known to be as critical micelle concentration CMC. For exact CMC determination, the plotted graph was included with the differential conductance corresponding to the concentration of surfactant, which showed a sigmoid-shaped curve (Figure 1).

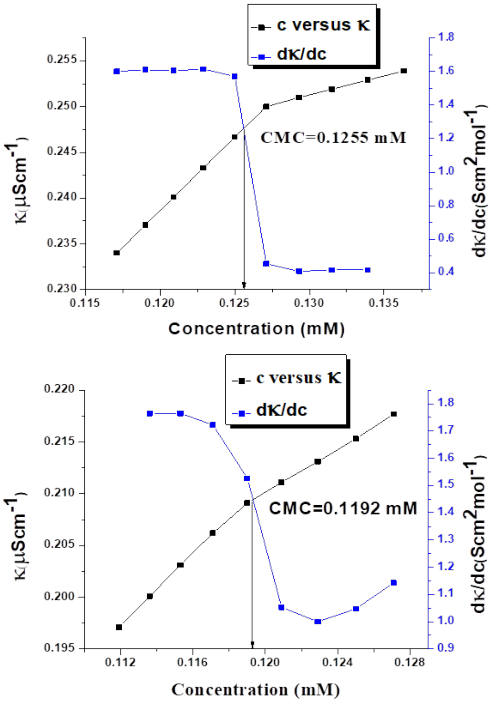

Fig. 1. The plots between conductivity (k) and differential conductivity (dk/dc) versus total concentration for the determination of CMC values for samples A1 (above) and A2 (below).

The graph shows that the conductance of the solution increases due to the excessive availability of free ions in the pre-micellar region of the surfactant solution. This is because, in the pre-micellar region, the molecules of the surfactant are in the form of monomers, which shows the presence of free cations and anions responsible for the increase in conductance value [42].

It was also observed that after reaching the post-micellar region of the surfactant, the conductance of the surfactant solution was lowered. The reason is that after the post miceller region, the free ions get captured by the micelle of the surfactant by incorporating inside the micelle and only the anion of the surfactant (Br^-) moves from one micelle to another. Therefore, the low conductance value is caused by the limited availability of free ions, which is represented on the graph as a sharp decline since they are all involved in the production of micelles [43, 44]. The CMC values of surfactants, A1 and A2, are 0.1255 and 0.1192 mM, respectively.

3.4. Determination of CMC by UV-Visible Absorption Spectroscopy

The absorption patterns of all the newly synthesized surfactant samples A1 and A2 are different, giving the critical micelle concentration (CMC) at different points. Unlike the CMC determination by using a conductometer, the CMC point identification was carried out by plotting a graph between concentration versus absorption and taking their differential values to avoid instrumental error. Whereas, λ_{max} determination of both samples A1 and A2 was carried out by the wavelength and absorption plot. The absorbance plots of samples A1 and A2 are shown in Figure 2. The CMC values of samples A1 and A2 are 0.1245 mM and 0.111 mM, respectively, which indicates that the CMC values calculated by both techniques are in the lower range which is beneficial for minimal toxicity by reducing the surfactant concentration.

3.5. Drug Interaction

The interaction of synthesized surfactants was also carried out with a standard drug ketoprofen (KP) (Figure S7). It has efficient anti-inflammatory activity and is also abbreviated as NSAID (non-steroidal anti-inflammatory drug) [45].

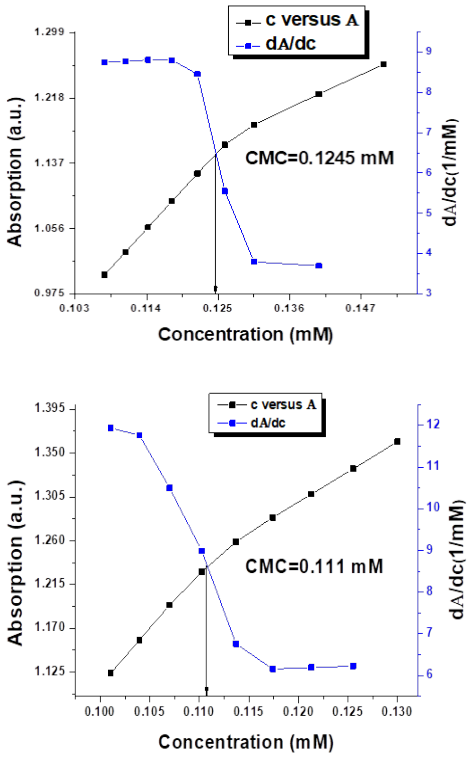

Fig. 2. The plots of Absorbance versus Concentration and the rate of change of absorbance with respect to concentration, showing the calculations of CMC values for samples A1 (above) and A2 (below).

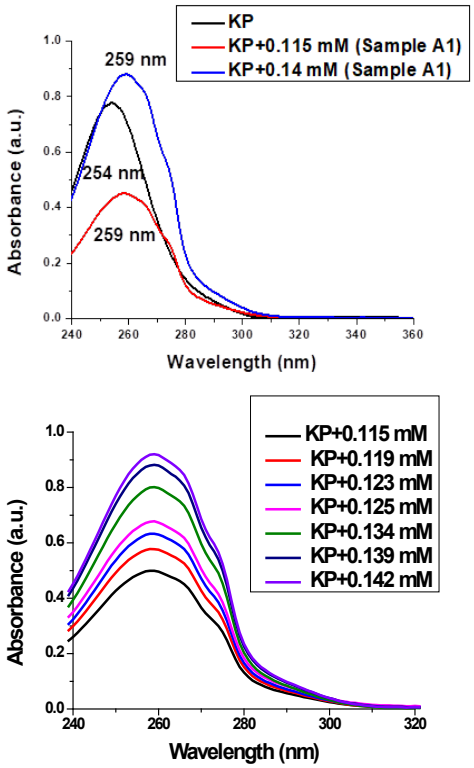

Fig. 3. Absorption spectra of KP; In the absence & presence of pre-micellar and post-micellar concentration of sample A1 (above) and with changing concentration of sample A1 (below).

3.5.1. Interaction of sample A1 with ketoprofen

The interaction pattern of newly synthesized surfactant sample A1 with the drug ketoprofen can be observed from the graphs as shown in Figure 3. As far as the absorption pattern of ketoprofen is concerned, it was noticed that the maximum absorption was at 254 nm. It was detected that when the drug was mixed with surfactant at pre-micellar concentration, a red shift of 5 nm was observed. In a post micellar region, an increase in drug absorption was observed, which depicts the enhancement of bio-availability and solubility of the drug. The premicellar and post-micellar concentrations of the sample with the drug are 0.115 mM and 0.14 mM, respectively [46, 47]. It was observed from the graphs that by increasing the concentration of surfactant, the absorption increases, which depicts the better solubilization of KP drug at 259 nm.

3.5.2. Interaction of sample A2 with ketoprofen

The interaction of ketoprofen with sample A2 shows almost the close pattern of absorption as that of sample A1 (Figure 4). The premicellar and post-micellar concentrations of the sample with the drug are 0.117 mM and 0.142 mM, respectively.

3.5.3. Calculations of Gibb's free energy and binding constant (K_b)

The interaction of samples A1, A2, and ketoprofen shows a straight-line pattern. For the sake of Gibb's free energy (ΔG) and binding constant (K_b) determination, a graph is plotted against 1/(Cs+Ca) versus 1/ΔA (Figure 5). The observed Gibb's free energy value was negative, which shows the reaction spontaneity between the ketoprofen and surfactant sample [48, 49].

As:

$$\Delta A = A^{o} - A$$

ΔA is the differential of absorbance.

A is the absorption of the drug at the same wavelength in the presence of surfactant.

A^{o} is the absorption of a drug in the absence of surfactant at its λ_{max}.

Ca is the concentration of the drug.

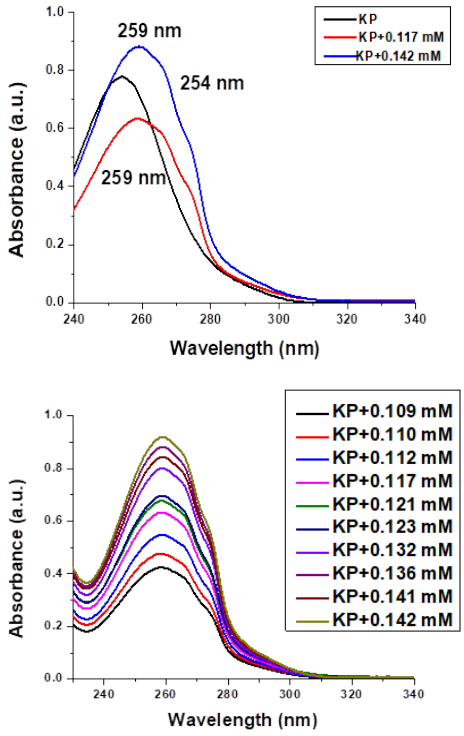

Fig. 4. Absorption spectra of KP; In the absence & presence of pre-micellar and post-micellar concentration of sample A2 (above) and with changing the concentration of sample A2 (below).

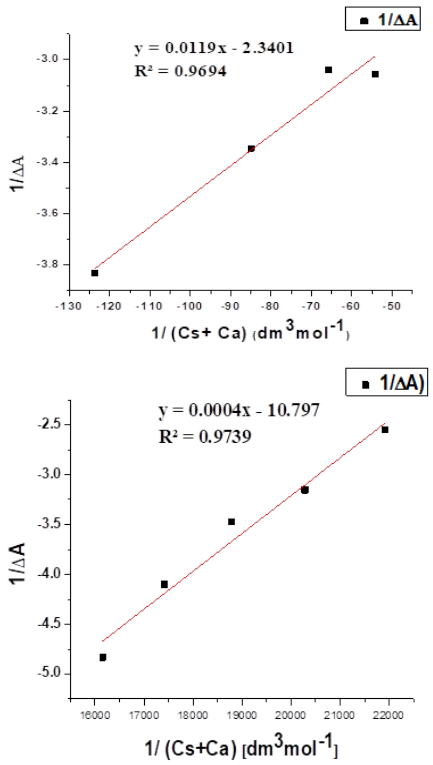

Fig. 5. Determination of binding constant (K_b) for samples A1 (above) and A2 (below).

Cs is the total surfactant concentration.
For sample A1,

We know the Lineweaver-Burk plot:
$1/\Delta A = m \cdot 1/(Cs + Ca) + b$
$y = mx + c$
slope (m) = 0.0119 [From Figure 5 (above)].
As, $m = 1/K$,
$K = 1/m = 1/0.0119 = 84.03\ M^{-1}$
(Also a binding constant $K_b = 84.03\ M^{-1}$)
We know that
$\Delta G = -RT \ln K$
$R = 8.314$ J/mol·K ; $T = 298$ K ; $K = 84.03\ M^{-1}$)

By putting the values in the Gibb's free energy equation, we get
$\Delta G = - (8.314 \text{ J/mol·K}) \cdot (298 \text{ K}) \cdot \ln(84.03)$
$\Delta G = - (8.314 \times 298) \cdot \ln(84.03)$
$\Delta G = - (2477.572) \cdot \ln(84.03)$
$\Delta G = - (2477.572) \cdot 4.430$
$\Delta G = -10995.6$ J/mol≈ -10.0 kJ/mol

The change in Gibb's free energy (ΔG) is -10.0 kJ/mol at room temperature (298 K).

For sample A2,

We know the Lineweaver-Burk plot:
$1/\Delta A = m \cdot 1/(Cs + Ca) + b$
$y = mx + c$
slope m = 0.0004 [From Figure 5. (below)]
As, $m = 1/K$,
$K = 1/m = 1/0.0004 = 2500\ M^{-1}$
(Also a binding constant $K_b = 2500\ M^{-1}$)
We know that
$\Delta G = -RT \ln K$
$R = 8.314$ J/mol·K ; $T = 298$ K ; $K = 2500\ M^{-1}$)
By putting the values in the Gibb's free energy equation, we get
$\Delta G = -19.37$ kJ/mol

The spontaneity of the binding process is referred to as the negative ΔG value. The greater the negative value, the higher will be the spontaneity and the stronger will be the binding. With the help of concentrations of surfactants and KP, followed by the absorbance of both samples of KP in the presence and absence of drug, the graph is plotted against the reciprocal of change in absorbance and the reciprocal of drug concentration and surfactant concentration.

Table 1. Inhibition zones of samples A1, A2, Gentamycin (standard drug), and ethanol (negative control) against different bacterial strains.

Bacterial strains	A1 (0.1 %)	A2 (0.1 %)	Gentamycin (Positive control) (0.1 %)	Ethanol (Negative control)
	Zones of inhibition (mm)			
Staphylococcus pseudo (Gram-positive)	7	5	6	6
Staphylococcus aureus (Gram-positive)	7	4	12	15
Klebsiella pneumoniae (Gram-negative)	5	3	5	10

The -ΔG for sample A1 and ketoprofen is 10.0 kJ/mol and for sample A2 and ketoprofen is 19.37 kJ/mol. The graph of sample A2 is plotted as same as sample A1 by the same calculations of absorbances and concentrations of surfactant and ketoprofen KP. Both the samples showed excellent activity with the drug and the best spontaneity of reaction. Ketoprofen showed efficient and almost the same patterned interaction regardless of Gibb's free value of both reactions.

3.6. Anti-bacterial Activities of Samples A1 and A2

The interaction of newly synthesized surfactant samples A1 and A2 was performed against *Staphylococcus pseudo, Klebsiella pneumoniae,* and *Staphylococcus aureus* bacterial strains and it was observed that the synthesized surfactants demonstrated limited inhibitory effects as reflected by the small zones of inhibitions observed (Figures S8-10, Table 1). The minimized result regarding the inhibition zones of the antibacterial activity may follow several reasons including the environmental factor involving the temperature and pH, and the invasion through the non-perforated bacterial outer membrane. For instance, Gram-negative bacteria exhibit likewise similar characteristics as discussed. Another reason, for the low antibacterial activity, may be the binding of the compound to the certain infected target, which may be owing to the hindrance in its structure, sterically. Some Gram-negative bacteria undergo the mutation which can be effectively responsible for the diversion of the antibiotic or a compound to another site, instead of the actual target, leading the compound least active toward the anti-bacterial activities [41, 50-52].

4. CONCLUSIONS

The unequivocal authentication for the newly synthesized pyridinium-based cationic surfactants, named N-(n-octadecyl)-2-methylpyridinium bromide (sample A1) and N-(n-octadecyl)-3-methylpyridinium bromide (sample A2), was investigated by FT-IR and NMR spectroscopic analysis. The aggregational behavior of the samples' monomers was manifested by the appreciable range of critical micelle concentration (CMC) values with the aid of conductometry and UV-visible spectroscopy. The efficient absorbance of the drug molecules to the samples' monomers was corroborated and authenticated by observing the absorbance patterns from pre-micellar to the post-micellar regions of the UV-visible spectrum during the sample-drug interaction. After micellization, the increased concentration of surfactant leads to more absorbance of the drug within the micelles of surfactant. The successful surpassing absorbance pattern of the drug-sample solution is remarking the pronounced bioavailability of the samples', leading it to the biomedical domain by augmenting its applicability. The cationic samples' binding capability and affinity with the anionic Ketoprofen drug encompass the substantial objective of the research work. The negative values of Ghibb's free energy for both compounds, calculated from the plots, depict the favorable spontaneity of the compounds. Moreover, both compounds are active toward the Gram-positive and negative bacterial strains, especially for the pronounced activity against *Staphylococcus aureus*. It is concluded that apart from the antibacterial activity, the synthesized samples with lower CMC values, are dynamically active towards the profound medical versatility as drug carriers.

5. CONFLICT OF INTEREST

The authors declare no conflict of interest.

6. ACKNOWLEDGEMENT

A.J. is thankful to Quaid-i-Azam University Islamabad for providing the facilities for this work. S.A. and A.H. thank the Pakistan Academy of Sciences and Quaid-i-Azam University, Islamabad for financial support.

7. REFERENCES

1. R. Aggarwal and S. Singh. Synthesis, self-aggregation, thermal stability, and cytotoxicity trends of alkyloxypropoxycyclohexane based pyridinium ionic liquids. *Journal of Molecular Liquids* 399: 124382 (2024).
2. P. Shenoy, N. Kedimar, and S.A. Rao. A comprehensive review on anticorrosive behaviour of surfactants across diverse metals using multiple techniques: Current insights and future horizons. *Chemical Engineering Journal Advances* 20: 100645 (2024).
3. B. Borikhonov, E. Berdimurodov, T. Kholikov, W.W. Nik, K.P. Katin, M. Demir, F. Sapaev, S. Turaev, N. Jurakulova, and I. Eliboev. Development of new sustainable pyridinium ionic liquids from reactivity studies to mechanism-based activity predictions. *Journal of Molecular Modeling* 30(11): 359 (2024).
4. S. Noori, A.Z. Naqvi, and W.H. Ansari. Experimental and Theoretical Approach to Cationic Drug-Anionic Gemini Surfactant Systems in Aqueous Medium. *Colloids and Surfaces B: Biointerfaces* 115: 71–78 (2014).
5. P. Werawatganone, and W. Muangsiri. Interactions between charged dye indicators and micelles to determine the critical micelle concentration. *Asian Journal of Pharmaceutical Sciences* 4: 221–227 (2009).
6. M.J. Rosen and J.T. Kunjappu (Eds.). 4th Edn.. Surfactants and Interfacial Phenomena. *John Wiley and Sons, New York* (2012).
7. P.A. Bhat, A.A. Dar, and G.M. Rather. Solubilization capabilities of some cationic, anionic, and nonionic surfactants toward the poorly water-soluble antibiotic drug erythromycin. *Journal of Chemical & Engineering Data* 53(6): 1271-1277 (2008).
8. T. Feng, H. Yang, J. Zhang, and C. Zong. Applicability of cationic surfactants, anionic surfactants, and nonionic surfactants as foaming agents for foamed concrete: surface activity, foamability, and interaction with cement. *Journal of Sustainable Cement-Based Materials* 13(9): 1330-1347 (2024).
9. P. Madaan and V.K. Tyagi. Quaternary pyridinium salts: a review. *Journal of Oleo Science* 57(4): 197-215 (2008).
10. R. Talat, M.A. Asghar, I. Tariq, Z. Akhter, F. Liaqat, L. Nadeem, H. Ali, and S. Ali. Evaluating the Corrosion Inhibition Efficiency of Pyridinium-Based Cationic Surfactants for EN_3B Mild Steel in Acidic-Chloride Media. *Coatings* 12(11): 1701 (2022).
11. A.O. Ezzat, A.M. Atta, and H.A. Al-Lohedan. Demulsification of stable seawater/Arabian heavy crude oil emulsions using star-like tricationic pyridinium ionic liquids. *Fuel* 304: 121436 (2021).
12. A.G. Hassabo, F. Saad, B.M. Hegazy, A. Sediek, and H. Ghazal. The use of cationic surfactants in the textiles industry. *Journal of Textiles, Coloration and Polymer Science* 20(2): 227-242 (2023).
13. D. Fu, X. Gao, B. Huang, J. Wang, Y. Sun, W. Zhang, K. Kan, X. Zhang, Y. Xie, and X. Sui. Micellization, surface activities and thermodynamics study of pyridinium-based ionic liquid surfactants in aqueous solution. *Royal Society of Chemistry Advances* 9(49): 28799-807 (2019).
14. F. Qin, Y. Zhang, K. Naseem, Z. Chen, G. Suo, W. Hayat, and S.H.S. Gardezi. Assessment of the importance and catalytic role of chromium oxide and chromium carbide for hydrogen generation via hydrolysis of magnesium. *Nanoscale* 16(41): 19518-19528 (2024).
15. F. Qin, K. Naseem, Z. Chen, G. Suo, and A. Tahir. Carbon nano-tube coated with iron carbide catalysis for hydrolysis of magnesium to generate hydrogen. *International Journal of Hydrogen Energy* 83: 1359-1369 (2024).
16. A.Z. Hezave, S. Dorostkar, S. Ayatollahi, M .Nabipour, and B. Hemmateenejad. Effect of different families (imidazolium and pyridinium) of ionic liquids-based surfactants on interfacial tension of water/crude oil system. *Fluid Phase Equilibria* 360:139-45 (2013).
17. L.L. Schramm, E.N. Stasiuk, and D.G. Marangoni. 2 Surfactants and their applications. *Annual Reports Section "C" (Physical Chemistry)* 99: 3-48 (2003).
18. R. Goel, S. Bhardwaj, and S. Bana. Pharmaceutical excipients. *Dosage Forms, Formulation Developments and Regulations* 1: 311-348 (2024).
19. Z. Sun, Y. Ji, H. Wang, J. Zhang, C. Yuan, M. Kang and H. Yin. Impact of hydroxyethyl headgroup on long-

chain quaternary ammonium cationic surfactants: Solubility, surface activities, self-assembly behaviors, and rheological properties. *Colloids and Surfaces A: Physicochemical and Engineering Aspects* 700: 134831 (2024).
20. F.I. El-Dossoki, M.A. Migahed, M.M. Gouda, and S.A.E.H.A. El-Maksoud. Aggregation behavior of newly synthesized Gemini cationic surfactants in absence and in presence of different inorganic salts in 15% DMSO–water solvent. *Scientific Reports* 14(1): 20351 (2024).
21. T. Majeed, T.I. Sølling, and M.S. Kamal. Foamstability: The interplay between salt-, surfactant-and critical micelle concentration. *Journal of Petroleum Science and Engineering* 187: 106871 (2020).
22. C.B. Farias, F.C. Almeida, I.A. Silva, T.C. Souza, H.M. Meira, F.R. de Cássia, J.M. Luna, V.A. Santos, A. Converti, I.M. Banat, and L.A. Sarubbo. Production of green surfactants: Market prospects. *Electronic Journal of Biotechnology* 51: 28-39 (2021).
23. I.F.D.L. Fuente, S.S. Sawant, K.W. Kho, N.K. Sarangi, R.C. Canete, S. Pal, and J.L. Rouge. Determining the Role of Surfactant on the Cytosolic Delivery of DNA Cross-Linked Micelles. *ACS Applied Materials & Interfaces* 16(33): 43400-43415 (2024).
24. R.A. Gonçalves, K. Holmberg, and B . Lindman. Cationic surfactants: A review. *Journal of Molecular Liquids* 375: 121335 (2023).
25. S.P. Moulik, A.K. Rakshit, and B. Naskar. Physical chemical properties of surfactants in solution and their applications: A comprehensive account. *Journal of Surfactants and Detergents 27*(6): 895-925 (2024).
26. G. Hertel and H. Hoffmann. Lyotropic nematic phases of double chain surfactants. *Trends in Colloid and Interface Science II* 76: 123-131 (1988).
27. Z. Zhang, H. Liu, D.G. Yu, and S.W. Bligh. Alginate-Based Electrospun Nanofibers and the Enabled Drug Controlled Release Profiles: A Review. *Biomolecules* 14(7): 789 (2024).
28. S.D. Santos, B. Medronho, T.D. Santos, and F.E. Antunes. Amphiphilic molecules in drug delivery systems. *Drug Delivery Systems: Advanced Technologies Potentially Applicable in Personalised Treatment* 4: 35-85 (2013).
29. J. Abildskov and J.P. O'Connell. Molecular thermodynamic modeling and design of microencapsulation systems for drug delivery. *Journal of Chemical & Engineering Data* 56: 1229-1237 (2011).
30. C.Y. Wang, H.O. Ho, L.H. Lin, Y.K. Lin, and M.T. Sheu. Asymmetric membrane capsules for delivery of poorly water-soluble drugs by osmotic effects. *International Journal of Pharmaceutics* 297(1-2): 89-97 (2005).
31. S.I. Palma, M. Marciello, A. Carvalho, S. Veintemillas-Verdaguer, M.M. del Puerto and A.C. Roque. Effects of phase transfer ligands on monodisperse iron oxide magnetic nanoparticles. *Journal of Colloid and Interface Science* 437: 147-155 (2015).
32. V.P. Torchilin. Structure and design of polymeric surfactant-based drug delivery systems. *Journal of Controlled Release* 73(2-3): 137-172 (2001).
33. M.A. Rub, and A.Z. Naqvi. Micellization of Mixtures of Amphiphilic Drugs and Cationic Surfactants: A Detailed Study. *Colloids and Surfaces B: Biointerfaces* 92: 16-24 (2012).
34. K. Naseem, N.A. Khan, and S.H. Safeer. Effect of Magnesium Doping to Reduce the Charge Reservoir Layer in $Cu_{0.5}Tl_{0.5}(Ba_{2-x}Mg_x)Ca_2Cu_3O_y$ (x = 0, 0.15, 0.25, 0.35) Superconductors. *Journal of Electronic Materials* 5: 2164-2170 (2021).
35. G. Socrates (Ed.). Infrared and Raman Characteristic Group Frequencies: Tables and Charts. Third Edition. *John Wiley & Sons* (2004).
36. D. Cook. Vibrational spectra of pyridinium salts. *Canadian Journal of Chemistry* 39(10): 2009-2024 (1961).
37. R.J. Clark, and C.S. Williams. The far-infrared spectra of metal-halide complexes of pyridine and related ligands. *Inorganic Chemistry Journal* (3): 350-357 (1965).
38. G.X. Zhao, B.Y. Zhu, Z.P. Dou, P. Yan, and J. X. Xiao. Effect of charge distribution along surfactant molecules on physico-chemical properties of surfactant systems. *Colloids and Surfaces A: Physicochemical and Engineering Aspects* 327(1-3): 122-126 (2008).
39. N.S. Gill, R.H. Nuttall, D.E. Scaife, and D.A. Sharp. The infra-red spectra of pyridine complexes and pyridinium salts. *Journal of Inorganic and Nuclear Chemistry* 18: 79-87 (1961).
40. A. Sager, S. Rahman, S.A. Imtiaz, Y. Zhang, A. Alodhayb, P.E. Georghiou, and M. Al-Gawati. Oxidative and Extractive Desulfurization of Fuel Oils Catalyzed by N-Carboxymethyl Pyridinium Acetate and N-Carboxyethyl Pyridinium Acetate Acidic Ionic Liquids: Experimental and Computational DFT Study. *American Chemical Society Omega* 9: 23121-24104 (2024).

41. S. Fayyaz, S. Ali, N. Khalid, A. Shah, and F. Ullah. One Pot Synthesis and Properties of Cationic Surfactants: n-Alkyl-3-Methylpyridinium Bromide. *Journal of Surfactants and Detergents* (4): 841-848 (2016).
42. T.Q. Liu and R. Guo. Influence of low cetyltrimethylammonium bromide concentration on the interactions and properties of hemoglobin with acyclovir. *Chinese Journal of Chemistry* 24(5): 620-626 (2006).
43. S.S. Shah, A. Saeed, and Q.M. Sharif, A study of micellization parameters and electrostatic interactions in micellar solution of sodium dodecyl sulfate. *Colloids and Surfaces A* 155(2-3): 405-412 (1999).
44. F.A. Shah, A.M. Khan, S. Sabir, and S. Ali. CTAB–tributylstannic [3-(3′, 4′-dichlorophenylamido) propanoate] interaction: a tool for predicting organotin (IV) complex–cell membrane interaction parameters. *Colloid and Polymer Science* 294(1): 87-94 (2016).
45. T.G. Kantor. Ketoprofen: a review of its pharmacologic and clinical properties. *Pharmacotherapy: The Journal of Human Pharmacology and Drug Therapy* 6(3): 93-102 (1986).
46. A.M. Khan and S.S. Shah. A UV-visible study of partitioning of pyrene in an anionic surfactant sodium dodecyl sulfate. *Journal of Dispersion Science and Technology* 29(10): 1401-1407 (2008).
47. H. Itoh, S. Ishido, M. Nomura, T. Hayakawa, and S. Mitaku. Estimation of the hydrophobicity in microenvironments by pyrene fluorescence measurements: n-β-octylglucoside micelles. *The Journal of Physical Chemistry* 100(21): 9047-9053 (1996).
48. B. Naseem, A. Sabri, A. Hasan, and S.S. Shah. Interaction of flavonoids within organized molecular assemblies of anionic surfactant. *Colloies and Surfaces B* 35(1): 7-13 (2004).
49. M.A. Awan and S.S. Shah. Hydrophobic interaction of amphiphilic hemicyanine dyes with cationic and anionic surfactant micelles. *Colloids and. Surfaces A* 122(1-3): 97-101 (1997).
50. H.A. Grema, Y.A. Geidam, G.B. Gadzama, J.A. Ameh, and A. Suleiman. Methicillin resistant Staphylococcus aureus (MRSA): a review. *Advances in Animal and Veterinary Sciences* 3(2): 79-98 (2015).
51. T.D. Tavares, J.C. Antunes, J. Padrão, A.I. Ribeiro, A. Zille, M.T.P. Amorim, F. Ferreira, and H.P. Felgueiras. Activity of specialized biomolecules against gram-positive and gram-negative bacteria. *Antibiotics* 9(6): 314 (2020).
52. X.Z. Li, P. Plésiat, and H. Nikaido. The challenge of efflux-mediated antibiotic resistance in Gram-negative bacteria. *Clinical Microbiology Reviews* 28(2): 337-418 (2015).